Eksakta : Berkala Ilmiah Bidang MIPA
VOLUME 27 NO 02 2026, pp 219-230
ISSN : Print 1411-3724 — Online 2549-7464
DOI : https://doi.org/10.24036/eksakta/vol27-iss02/676

Eksakta
Berkala Ilmiah Bidang MIPA
http://www.eksakta.ppj.unp.ac.id/index.php/eksakta

Article

In Silico Evaluation of Cardiac Glycosides from *Vernonia amygdalina* as EGFR Inhibitors in Triple Negative Breast Cancer

Gisela Agustin Habayahan[1], Denny Satria[1*]

[1]Department of Pharmaceutical Biology, Faculty of Pharmacy, Universitas Sumatera Utara, Medan, Indonesia

Article Info

Article history :
Received April 15, 2026
Revised April 25, 2026
Accepted April 29, 2026
Published April 30, 2026

Keywords :
Cardiac glycosides,
EGFR, in silico,
triple negative breast cancer,
Vernonia amygdalina,

Abstract. Triple-negative breast cancer (TNBC) is an aggressive subtype with limited targeted therapies, emphasizing the urgent need for novel molecular inhibitors. Epidermal growth factor receptor (EGFR) is overexpressed in TNBC, but current inhibitors show limited clinical efficacy, indicating a significant therapeutic gap. This study aims to evaluate cardiac glycosides from *Vernonia amygdalina* as EGFR inhibitors using an integrated in silico approach. Docking results demonstrated that vernoniosides A3 exhibited the lowest binding energy of -12.2 kcal/mol, outperforming the native ligand (-9.0 kcal/mol) and gefitinib (-8.5 kcal/mol). Molecular dynamics (MD) simulations revealed that EGFR-vernoniosides A3 complex remained stable, with RMSD values within stable range (0.7-3.8 Å), RMSF values (0.4-8.3 Å), radius of gyration (Rg) (6.0-7.0 Å), solvent-accessible surface area (SASA) (830-871 Å²), while forming up to 15 hydrogen bonds. However, MM-PBSA analysis showed that binding free energy of vernoniosides A3 (321.60 ± 5084.43 kcal/mol) was lower than the native ligand (569.25 ± 8997.10 kcal/mol) and gefitinib (623.87 ± 9862.73 kcal/mol), indicating weaker thermodynamic binding strength. This discrepancy arises as docking measures potential binding in a static state, while MM-PBSA reflects dynamic, realistic binding strength. These results suggest that vernoniosides A3 shows promising binding affinity but requires further optimization and validation for TNBC therapy.

Corresponding Author :
Denny Satria
Department of Pharmaceutical Biology, Faculty of Pharmacy,
Universitas Sumatera Utara, Medan , Indonesia
Email : dennysatria@usu.ac.id

1. Introduction

Breast cancer is one of the deadliest neoplasms with approximately 2.3 million cases diagnosed globally in 2022 [1]. Triple-negative breast cancer (TNBC) is the most aggressive subtype of the breast cancer subtypes due to the loss of expression of estrogen receptor (ER)/progesterone receptor (PR) or human epidermal growth factor 2 (HER2), and it also has limited effective treatment options [2]. It has features of high proliferation rate, higher metastasis potential and the risk of recurrence is more than other subtypes [3]. The epidermal growth factor receptor (EGFR) has been investigated as one of the potential molecular targets in TNBC, due to its overexpression and significance in cancer cell proliferative capacity, survival and metastasis [4-5]. EGFR is found to be overexpressed in TNBC [6-7]. Several EGFR inhibitors, such as gefitinib and erlotinib, have been developed as targeted therapies [8-9]. However, the clinical efficacy of these inhibitors in TNBC remains limited, making it necessary to identify alternative compounds that are more effective.

Vernonia amygdalina (VA) is a traditional medicinal plant that has been demonstrated to exhibit different pharmacological activities, including antibacterial [10], anticholesterol [11], antioxidant [12], anti-inflammatory [13] and anticancer activity [14-17]. Previous computational studies have shown that the cardiac glycoside VA has a high affinity for the p110α subunit of PI3K [18]. In HER2-positive breast cancer cells, it can induce apoptosis and block the cell cycle by targeting ERBB2, ESR1, EGFR, PIK3CA and PTPN11 [19]. In silico approaches are widely used in drug discovery because they can efficiently predict ligand-protein interactions and evaluate complex stability. However, no studies have evaluated the potential of VA cardiac glycosides as EGFR inhibitors using a combination of molecular docking and molecular dynamics simulations.

This study aims to fill this gap by employing an integrated in silico approach, combining molecular docking and molecular dynamics simulations to evaluate the potential of VA cardiac glycosides as EGFR inhibitors for TNBC. The novelty of this study lies in its use of combined methods to assess binding affinity and stability, targeting TNBC, a subtype with significant treatment challenges. The hypothesis is that cardiac glycosides from Vernonia amygdalina can inhibit EGFR in TNBC through stabilization of the ligand-receptor complex, paving the way for the development of new therapies for TNBC.

2. Experimental Section

2.1. Materials

In this study, EGFR receptor (PDB ID: 5UG8), downloaded from the Protein Data Bank (PDB) (https://www.rcsb.org). VA isolation obtained a biological activity with cardiac glycosides compounds as ligands. These six compounds are vernoamyosides A-D, vernocuminosides G, vernoniamyosides A-D, vernoniosides A1-A4, vernoniosides B1-B3, and vernonioside D. Based on these reports, data were collected to obtain SMILES codes for each VA cardiac glycosides compound. The 2D chemical structures of each compound were drawn using ChemDraw Pro 8.0 28. The created structures were converted into SMILES code and formatted for storage in PDB. The software used included ChemDraw Pro 8.0, AutoDock Tools 1.5.7, AutoDock Vina, PyMOL, BIOVIA Discovery Studio 2021, and YASARA 23.9.29. Computations were performed using an Acer Aspire Lite 14 (Intel® N100, 8 GB RAM) and a high-performance computer with an Intel® Xeon® E5-2699 v3 processor and 128 GB RAM.

2.2 Procedure

2.2.1 Ligand Preparation and Optimization

The ligand structure was created using ChemDraw in .mol format, then converted to .pdb format using Biovia Discovery Studio. Next, the ligand was optimized in AutoDock Tools by adding gasteiger charges and polar hydrogens, removing non-polar hydrogens, adjusting torsional angles, and saved in .pdbqt format.

2.2.2 Protein Preparation and Optimization

The three-dimensional structure of epidermal growth factor receptor (EGFR) (PDB ID: 5UG8) was obtained from the Protein Data Bank. Water molecules, unnecessary residues, and the native ligand were removed using Biovia Discovery Studio Visualizer. The protein was then prepared using AutoDock Tools by adding gasteiger charges and polar hydrogen atoms, while nonpolar hydrogens were merged. The final structure was saved in .pdbqt format for molecular docking.

2.2.3 Molecular Docking Validation

The validation procedure was performed using the native ligand of the EGFR protein (PDB ID: 5UG8). The active site was defined using a 28 × 28 × 28 grid box centered at coordinates (x = −13.156, y = 15.092, z = −25.718) using AutoDock Vina. The native ligand was then redocked to the binding site to assess the accuracy of the docking protocol. The docking process was performed using the commands vina.exe --config config.txt and vina_split.exe --input with the same grid box. The RMSD values between the redocked ligand and the original ligand were calculated using PyMOL to ensure docking accuracy. The docking results were then visualized by opening the ligand-bound receptor using Biovia Discovery Studio.

2.2.4 Molecular Dynamics Simulation

Molecular dynamics simulations were performed using YASARA to evaluate the stability of the protein-ligand complexes under physiological conditions. The selected docking complexes were prepared by adjusting the system to pH 7.4 and removing unnecessary molecules. The simulations were conducted using the AMBER force field at a temperature of 310 K for a duration of 100 ns. Structural stability was analyzed using RMSD, RMSF, radius of gyration (Rg), solvent-accessible surface area (SASA), hydrogen bond and Molecular Mechanics Poisson-Boltzmann Surface Area (MM-PBSA).

2.2.5 MM-PBSA Calculation

Trajectory analysis was performed using the YASARA script, and snapshots were used to calculate binding free energy via MM-PBSA with the AMBER14 force field. Higher positive energy values indicate stronger binding affinity, while the PBSA model accounts for solvation effects in the stability of the protein-ligand complex. The binding free energy was calculated using the following formula:

Binding free energy = E_potReseptor + E_solvReseptor + E_potLigand + E_solvLigand - E_potKompleks - E_solvKompleks

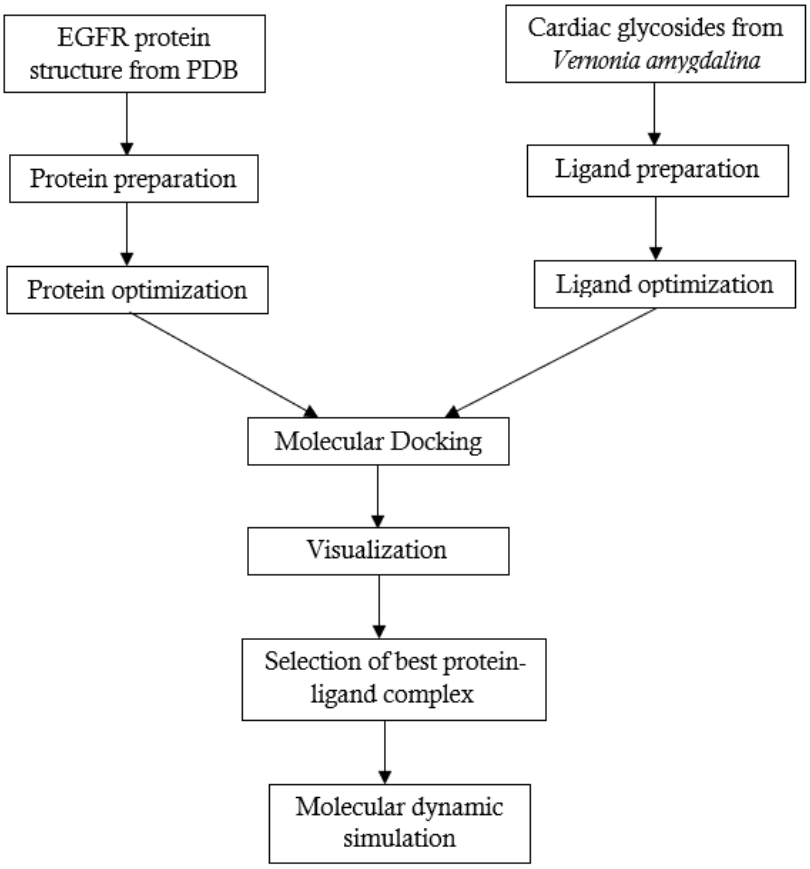

Figure 1. Molecular docking dan dynamic procedure

3. Results and Discussion

The protein's active site was analyzed where the RMSD values for was 1.997 Å. RMSD value of less than 2 Å is generally considered good. This parameter is used to evaluate the ability of a docking method to reproduce ligand-binding positions by comparing the ligand poses with the experimental crystal structure. The lower the RMSD value obtained, the higher the level of fit and accuracy of the docking results [20].

Table 1. The docking affinity of compounds binding to the protein target

Compounds	Binding Affinity (kcal/mol)	Interaction with amino acid	
		Hydrogen Bond	Hydrophobic and others interaction
Native ligand (8BP)	-9.0	Asn842, Met793, Leu718,	Phe723, Ser720, Gly719, Thr854, Met790, Leu792, Gly796, Cys797, Arg841, Val726, Leu844, Phe856, Lys745, Ala743
Gefitinib	-8.5	Cys797, Asp800, Pro794	Gly719, Phe723, Asn842, Leu792, Gly796, Thr854, Gln791, Lys745, Phe856, Val726, Ala743, Cys775,

			Met790, Leu844, Met793, Leu718, Arg841
Vernoamyosides A	-9.6	Cys797, Arg803, Asp800	Trp880, Lys913, Pro914, Glu906, Leu799, Ser720, Gly719, Leu718, Gly796, Pro794, Leu792, Thr854, Gln791, Cys775, Phe723, Ala743, Arg841, Val726, Lys745, Met790, Met793, Leu844, Phe856
Vernoamyosides B	-11.2	Met793, Arg803,	Ser720, Phe723, Gly719, Leu844, Lys745, Val726, Thr854, Ala743, Met790, Gln791, Leu792, Leu718, Gly796, Asn842, Leu799, Cys797, Arg841, Lys913, Pro914, Phe856, Trp880
Vernoamyosides C	-10.6	Lys745, Met793, Arg803, Gln791, Thr854, Phe856	Leu799, Phe723, Ser720, Gly719, Gly796, Leu844, Leu718, Leu792, Ala743, Cys775, Met790, Asp855, Lys913, Pro914, Val726, Cys797, Arg841, Trp880
Vernoamyosides D	-10.0	Thr854, Gln791, Met793	Glu906, Trp880, Pro914, Lys913, Leu799, Arg803, Asn842, Leu718, Leu792, Ala743, Cys775, Met790, Lys745, Gly719, Phe723, Ser720, Val726, Cys797, Arg841, Leu844, Phe856
Vernocuminosides G	-9.1	Ser720, Ala722, Lys745, Met793, Arg841, Asp837, Gln791, Thr854, Gly721, Phe856	Pro877, Phe723, Asn842, Gly719, Asp855, Met790, Cys775, Leu844, Ala743, Gly796, Leu792, Leu718, Val726, Cys797,
Vernoniamyosides A	-10.3	Met793, Arg803, Arg841, Gln791, Lys913	Trp880, Glu906, Pro914, Leu799, Asn842, Gly796, Leu718, Leu792, Ala743, Met790, Lys745, Leu844, Thr854, Val726, Gly719, Phe723, Ser720, Cys797, Phe856
Vernoniamyosides B	-10.0	Lys745, Met793, Arg841, Gln791, Thr854, Phe856	Leu799, Lys913, Arg803, Trp880, Gly796, Leu844, Ala743, Leu792, Cys775, Met790, Phe723, Gly719, Ser720, Leu718, Val726, Cys797
Vernoniamyosides C	-10.7	Cys797, Arg841, Asp837	Gly719, Gly796, Leu718, Leu792, Ala743, Met793, Gln791, Cys775, Thr854, Leu844, Asn842, Phe723,

			Gly721, Pro877, Val726, Lys745, Met790, Phe856
Vernoniamyosides D	-10.8	Arg841, Asp837, Gly796	Gly719, Leu718, Met793, Ala743, Leu792, Gln791, Cys775, Thr854, Leu844, Asn842, Phe723, Gly721, Pro877, Cys797, Val726, Lys745, Met790, Phe856
Vernoniosides A1	-10.3	Arg841	Trp880, Gly719, Gly796, Leu718, Gln791, Ala743, Leu792, Thr854, Phe723, Asn842, Gly721, Asp837, Pro877, Cys797, Cys775, Met793, Leu844, Val726, Lys745, Met790, Phe856
Vernoniosides A2	-10.3	Arg841	Trp880, Pro877, Asp837, Gly719, Gly796, Leu792, Ala743, Gln791, Lys745, Thr854, Leu718, Phe723, Gly721, Asn842, Cys797, Cys775, Met793, Leu844, Val726, Met790, Phe856
Vernoniosides A3	-12.2	Asp837	Arg858, Pro877, Arg841, Ser720, Gly719, Leu718, Gly796, Met793, Leu844, Gln791, Leu792, Cys797, Asn842, Gly721, Ala722, Ala743, Cys775, Met790, Val726, Lys745, Phe723, Phe856
Vernoniosides A4	-10.5	Met793, Arg803, Arg841, Gly796, Gln791	Pro914, Ser720, Phe723, Gly719, Leu844, Val726, Thr854, Met790, Ala743, Leu792, Leu718, Asn842, Asp800, Leu799, Cys797, Lys913, Phe856, Trp880
Vernoniosides B1	-10.6	Arg841, Asp837, Arg858	Pro877, Asn842, Cys797, Leu844, Leu792, Thr854, Gln791, Met793, Lys745, Leu718, Gly796, Gly719, Ser720, Gly721, Ala722, Ala743, Cys775, Met790, Val726, Phe723, Phe856
Vernoniosides B2	-10.2	Lys745, Met793, Gln791, Thr854, Phe856	Leu799, Trp880, Lys913, Asn842, Gly796, Leu718, Leu844, Leu792, Ala743, Cys775, Met790, Gly719, Phe723, Ser720, Val726, Cys797, Arg841
Vernoniosides B3	-9.4	Arg841	Asn842, Thr854, Ala743, Phe795, Pro794, Leu792, Gly796, Met793,

			Gly719, Trp880, Leu799, Arg803, Lys913, Cys797, Leu844, Val726, Leu718, Phe856
Vernoniosides D	-11.5	Met793, Arg803, Asp800, Gln791	Ser720, Phe723, Gly719, Lys745, Leu844, Val726, Thr854, Met790, Ala743, Leu792, Leu718, Gly796, Asn842, Leu799, Cys797, Arg841, Lys913, Pro914, Phe856, Trp880
Vernoniosides D2	-11.2	Met793, Arg803, Gln791,	Glu906, Pro914, Asp800, Asn842, Lys745, Leu844, Ala743, Leu792, Gly796, Leu718, Val726, Gy719, Phe723, Ser720, Cys797, Arg841, Leu799, Lys913, Phe856, Trp880
Vernoniosides E	-9.6	Ala722, Met793, Arg841, Gln791, Thr854	Asp837, Gly721, Ser720, Asn842, Gly719, Leu718, Lys745, Cys775. Met790, Leu844, Ala743, Leu792, Pro877, Val726, Cys797, Phe723, Phe856

When the binding affinity value is lower, the ligand-target protein connection is more robust and durable [21]. Based on the Table 1, in comparison to the native ligand (-9.0 kcal/mol) and gefitinib (-8.5 kcal/mol), the vernoniosides A3 compound exhibited the lowest bindng affinity value for the EGFR protein, at -12.2 kcal/mol, followed by the vernoniosides D compound.

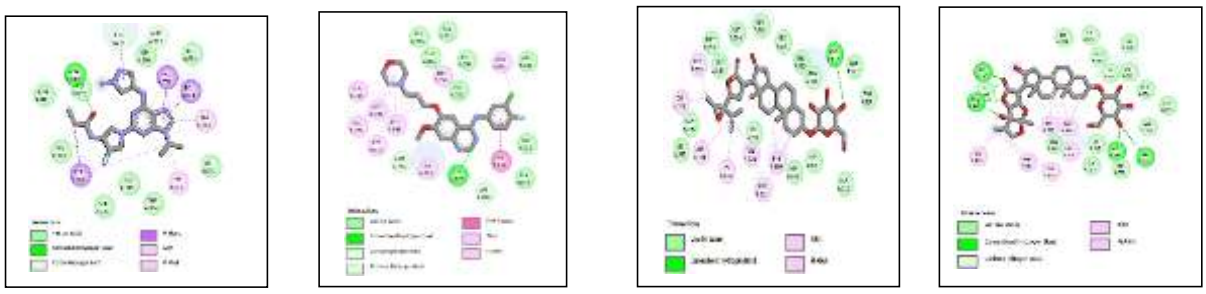

(A) (B) (C) (D)

Figure 2. 2D visualizations of the molecular docking interaction. (A) EGFR – Native Ligand (8BP); (B) EGFR – Gefitinib; (C) EGFR – Vernoniosides A3; (D) EGFR – Vernoniosides D

At the EGFR target (5UG8), vernoniosides A3 and D, showed consistent interactions with six key residues in the EGFR kinase domain, Met790, Val726, Phe723, Arg858, Phe856, and Cys797 as shown in Figure 2 [22]. Val726 is the most frequently interacting residue in the crystal structure and is part of the hinge region. This residue forms a highly hydrophobic core binding pocket [23]. The hydrophobic contact between the aromatic ring group of the ligand and Phe856 may influence the allosteric activity. Ligand binding at the allosteric site can inhibit autophosphorylation of the kinase domain and maintain the stability of the protein's structural structure [24].

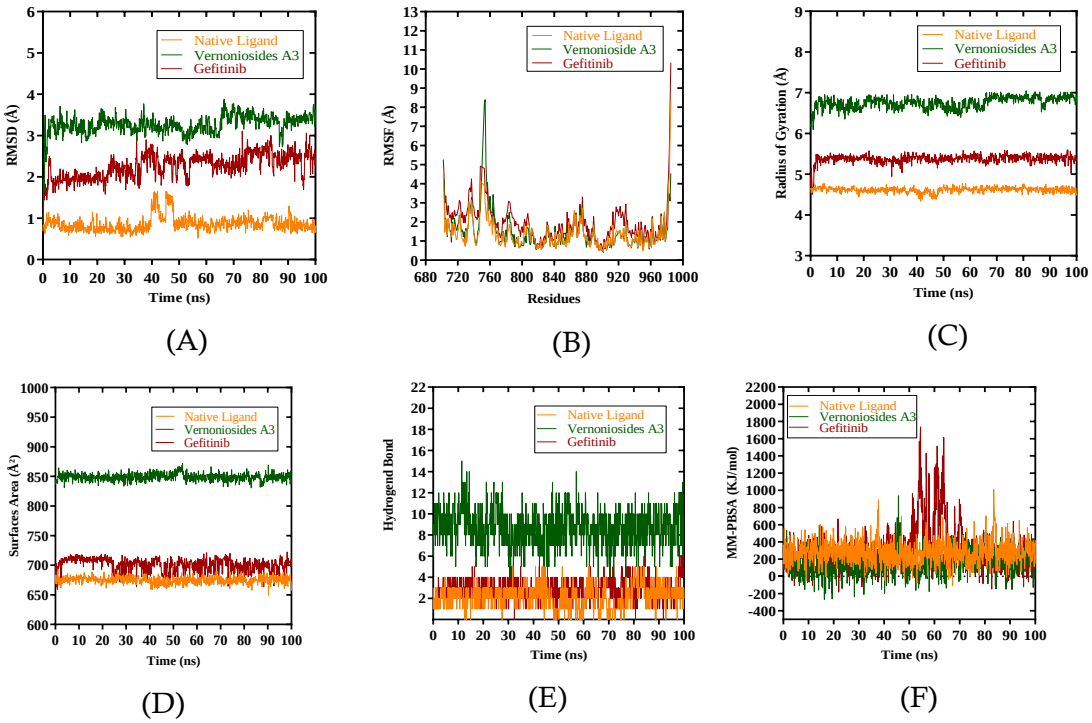

Figure 3. Visualization of EGFR-vernoniosides A3 target molecular dynamics simulation

The dynamic behavior and conformational ligand-protein complexes under physiologically relevant conditions were investigated using molecular dynamics modelling. RMSD was used to assess structural deviations of the complexes during the simulation, where stable values generally indicate conformational stability and sustained ligand binding [25].

As shown in Figure 3(A), the EGFR-vernoniosides A3 complex exhibited slightly higher RMSD values than the native ligand and gefitinib, within stable range 0.7-3.8 Å. Although the vernoniosides A3 value is higher, the RMSD curve reaches a stable plateau without a progressive upward trend over 100 ns, indicating that the complex remains in a state of conformational equilibrium after the initial equilibration phase, thereby supporting the assumption of structural stability [26]. The slightly higher RMSD value for the vernoniosides A3 compound can be explained by its larger molecular size and the internal flexibility of the ligand. Large ligands often force the kinase domain to adjust its local structure to accommodate the interaction, while the fact that the RMSD value does not increase progressively still reflects the core stability of the active site [27].

RMSF analysis was used to assess the degree of residue flexibility during the simulation process. RMSF analysis, as shown in Figure 3(B), indicates that the protein residues in both complexes exhibit fluctuation values below 10 Å, suggesting stable dynamic flexibility [28]. RMSF analysis is used to assess the flexibility of protein residues during molecular dynamics simulations, which can influence the stability and orientation of ligands within the active site. For the EGFR-vernoniosides A3 complex, RMSF values ranged from 0.406 to 8.397 Å, with an average of 1.44 Å. Residues around the active site, including Met790, Val726, Phe723, Arg858, Phe856, and Cys797, exhibited low RMSF values (<2.5 Å), indicating that the core structure of the kinase domain remains stable and the ligand maintains optimal orientation for critical interactions [26].

Higher RMSF fluctuations are observed at the N-terminal and C-terminal ends of the protein, which is a common phenomenon in dynamics simulations because the terminal regions are more

exposed to the solvent and less stabilized by secondary structure [29]. In contrast, residues in the core region of the protein, particularly in the ligand-binding domain, exhibited lower RMSF values and greater stability, indicating that the EGFR-vernoniosides A3 complex does not induce significant structural changes. Loop and coil regions outside the rigid secondary structure tend to be more flexible, resulting in higher RMSF values, while residues around the active site remain stable due to ligand binding and movement restrictions imposed by the more rigid secondary structure [30-31].

Rg analysis assessed protein compactness during the simulation. In the EGFR-vernoniosides A3 complex as shown in Figure 3(C), it was found that vernoniosides A3 had a slightly higher Rg value than the native ligand and gefitinib. For the EGFR-vernoniosides A3 complex, Rg ranged from 6.0 to 7.0 Å indicating that the protein undergoes local relaxation to accommodate the large ligand. This increase in Rg is not a sign of overall protein instability but rather an adaptive response of the protein, in which more flexible loops and coils adjust to allow the ligand to bind optimally without disrupting the core structure of the kinase domain [32]. Moderate fluctuations in Rg indicate that the protein maintains global stability while making the local adjustments necessary for ligand interaction [33]. Biologically, this adaptation allows the ligand to remain in an optimal position to interact with key residues, supporting the potential for EGFR inhibition.

SASA is a measure of the surface area of a protein or protein-ligand complex that is accessible to solvent molecules, typically water, and is used to evaluate the extent to which a protein-ligand complex is compact or open. SASA analysis of MD simulations showed that the EGFR-vernoniosides A3 complex had an average value of 848.769 Å², higher than that of the native ligand 674.902 Å² and gefitinib 700.587 Å². This increase in SASA reflects that the protein adjusts its local conformation, particularly in the loops and terminal residues, thereby exposing more of its surface to the solvent [34]. Protein loops and terminal residues are naturally more flexible than the protein core, so this movement exposes additional surface area while still allowing ligand binding, which explains the increased SASA [33].

Hydrogen bond analysis was performed to assess the contribution of intermolecular interactions to the stability of protein-ligand complexes during MD simulations. The EGFR-vernoniosides A3 complex consistently formed more hydrogen bonds (15 per frame) than the native ligand (5) and gefitinib (7), indicating higher local stability of the complex. The EGFR-vernoniosides A3 complex consistently forms more hydrogen bonds than the native ligand and gefitinib. This can be explained by the local flexibility of the protein, particularly in the loops and terminal residues, which allows the ligand to occupy an optimal position so that more donor and acceptor atoms are within the proper distance to form hydrogen bonds [35]. Additionally, the ligand's orientation at the active site and small fluctuations during the simulation allow for the dynamic formation of additional hydrogen bonds. Consequently, the complex becomes more locally stable because these interactions lock the ligand in the active site and reduce its mobility [36].

With the MM-PBSA method via YASARA, a larger (more positive) single value for bond energy indicates one strong binding affinity and the ability of this complex to remain stable. The interaction bond energy values of the EGFR-vernoniosides A3 complex was 321.60 ± 5084.43 kcal/mol (Figure 3F), which was lower than those of native ligand (569.25 ± 8997.10 kcal/mol) and the reference drug (623.87 ± 9862.73 kcal/mol). Meanwhile, the initial docking scores indicate the highest affinity for vernoniosides A3. This discrepancy highlights a contradiction between the two methods, although docking predicts the best pose and high binding energy, MM-PBSA provides a more conservative estimate of the free energy. This phenomenon can be explained because docking uses a static scoring function that evaluates interactions based on the initial conformations of the ligand and protein, without accounting for protein flexibility, fluctuations in loop or terminal residues, solvation effects, and entropy contributions that arise during simulation [37].

In contrast, MM-PBSA evaluates the free energy of an ensemble of poses during the simulation, including dynamic non-covalent interactions and implicit solvent effects, thereby providing a more realistic picture of the complex's stability. Although the MM-PBSA energy for vernoniosides A3 is lower, the complex remains stable during the simulation because the ligand maintains hydrogen bonds and key interactions at the active site [38].

4. Conclusion

The docking studies revealed that most of the compounds had a higher binding affinity than native ligand and gefitinib, whereas vernoniosides A3 displayed the lowest binding energy. The EGFR-vernoniosides A3 complex remained acceptable stability by molecular dynamics simulation as indicated via RMSD, RMSF, Rg, SASA and hydrogen bond. However, MM-PBSA results demonstrated that the binding strength of the compound was still lower than that of the reference ligand. These results indicate that vernoniosides A3 being a new candidate, ideally, need to be explored further although additional experimental validation is needed.

References

[1] Bray, F., Laversanne, M., Sung, H., Ferlay, J., Siegel, R.L., Soerjomataram, I., et al. (2024). Global cancer statistics 2022: GLOBOCAN estimates of incidence and mortality worldwide for 36 cancers in 185 countries. CA Cancer J Clin, 74(3), 229-263.

[2] Obidiro, O., Battogtokh, G., Akala, E. O. (2023). Triple Negative Breast Cancer Treatment Options and Limitations: Future Outlook. Pharmaceutics, 15(7). 1-26.

[3] Li, X., Yang, J., Peng, L., Sahin, A. A., Huo, L., Ward, K. C., et al. (2016). Triple-negative breast cancer has worse overall survival and cause-specific survival than non-triple-negative breast cancer. Breast Cancer Res Treat, 161(2), 279-287.

[4] Yamaoka, T., Ohba, M., Ohmori, T. (2017). Molecular-targeted therapies for epidermal growth factor receptor and its resistance mechanismse. Int J Mol Sci, 18(11), 1-22.

[5] Sharma, B., Singh, V. J., Chawla, P. A. (2021). Epidermal growth factor receptor inhibitors as potential anticancer agents: An update of recent progress. Bioorg Chem, 116, 1-29.

[6] Hashmi, A. A., Naz, S., Hashmi, S. K, Irfan, M., Hussain, Z. F., Khan, E. Y., et al. (2019). Epidermal growth factor receptor (EGFR) overexpression in triple-negative breast cancer: association with clinicopathologic features and prognostic parameters. Surgical and Experimental Pathology, 2(6), 1-7.

[7] Gluz, O., Liedtke, C., Gottschalk, N., Pusztai, L., Nitz, U., Harbeck, N. (2009). Triple-negative breast cancer - Current status and future directions. Annals of Oncology, 20(12), 1913-1927.

[8] Cohen, M. H., Williams, G. A., Sridhara, R., Chen, G., Pazdur, R. (2003). FDA Drug Approval Summary: Gefitinib (ZD1839) (Iressa ®) Tablets. Oncologist, 8(4), 303-306.

[9] Cohen, M. H., Johnson, J. R., Chen, Y. F., Sridhara, R., Pazdur, R. (2005). Regulatory Issues-FDA FDA Drug Approval Summary: Erlotinib (Tarceva ®) Tablets. Oncologist, 10(7), 461-466.

[10] Sarijowan, T. P. D., Bodhi, W., Lebang, J. S. (2022). Uji Aktivitas Antibakteri Daun Afrika Terhadap Pertumbuhan Bakteri Staphylococcus aureus dan Pseudomonas aeruginosa. PHARMACON, 11(4), 1678-1685.

[11] Yani, N dan Thristy, I. (2021). Perbandingan Efektifitas Ekstrak Etanol Daun Afrika (Vernonia amygdalina Del) Dengan Simvastatin Terhadap Kadar Trigliserida Tikus Jantan Galur Wistar Yang Diinduksi Kuning Telur. JURNAL PANDU HUSADA, 2(1), 1-7.

[12] Wang, W. T., Liao, S. F., Wu, Z. L., Chang, C. W., Wu, J. Y. (2020). Simultaneous study of antioxidant activity, DNA protection and anti-inflammatory effect of Vernonia amygdalina leaves extracts. PLoS One, 15(7), 1-17.

[13] Pham, E. C., Doan, V. V., Thi, T. V. L., Ngo, C. V., Van, L. V. (2024). In vivo and in silico antihypertensive, anti-inflammatory, and analgesic activities of Vernonia amygdalina Del. leaf extracts. Heliyon, 10(19), 1-26.
[14] Lifiani, R., Harahap, U., Hasibuan, P. A. Z., Satria, D. (2018). Anticancer effect of african leaves (Vernonia amygdalina del.) to T47D cell resistant. Asian Journal of Pharmaceutical and Clinical Research, 11(1), 4-7.
[15] Hasibuan, P. A. Z., Harahap, U., Sitorus, P., Satria, D. (2020). The anticancer activities of Vernonia amygdalina Delile. Leaves on 4T1 breast cancer cells through phosphoinositide 3-kinase (PI3K) pathway. Heliyon, 6(7), 1-5.
[16] Satria, D., Hasibuan, P. A. Z., Muhammad, M., Waruwu, S. B., Utomo, R. Y., Ghoran, S. H. (2024). Cytotoxic and apoptotic effect of Vernonia amygdalina Delile. fractions against Hs578t triple-negative breast cancer cell lines. Phytomedicine Plus, 4(4), 1-8.
[17] Hasibuan, P. A. Z., Sitorus, R. K. U. A. B., Hermawan, A., Huda, F., Waruwu, S. B., Satria, D. (2024). Anticancer activity of the ethylacetate fraction of Vernonia amygdalina Delile towards overexpression of HER-2 breast cancer cell lines. Pharmacia, 71, 1-8.
[18] Tafrihani, A. S., Hanif, N., Yoga, I. M. B. K., Irmasari, I., Fakih, T. M., Novitasari, D., et al. (2025). A computational study of cardiac glycosides from Vernonia amygdalina as PI3K inhibitors for targeting HER2 positive breast cancer. J Comput Aided Mol Des, 39(1), 1-13.
[19] Hermawan, A., Satria, D., Hasibuan, P. A. Z., Huda, F., Tafrihan, A. S., Fatimah, N., et al. (2024). Identification of potential target genes of cardiac glycosides from Vernonia amygdalina Delile in HER2+ breast cancer cells. South African Journal of Botany, 164, 401-418.
[20] Libera, J. L. V., Verdugo, F. D., Jiménez, A. V., Vivanco, G. N., Caballero, J. (2020). LigRMSD: A web server for automatic structure matching and RMSD calculations among identical and similar compounds in protein-ligand docking. Bioinformatics, 36(9), 2912-2914.
[21] Fadlan, A., Nusantoro, Y. R. (2021). The Effect of Energy Minimization on The Molecular Docking of Acetone-Based Oxindole Derivatives. JKPK (Jurnal Kimia Dan Pendidikan Kimia), 6(1), 69-77.
[22] Planken, S., Behenna, D. C., Nair, S. K., Johnson, T. O., Nagata, A., Almaden, C., et al. (2017). Discovery of N-((3R,4R)-4-Fluoro-1-(6-((3-methoxy-1-methyl-1H-pyrazol-4-yl)amino)-9-methyl-9H-purin-2-yl)pyrrolidine-3-yl)acrylamide (PF-06747775) through Structure-Based Drug Design: A High Affinity Irreversible Inhibitor Targeting Oncogenic EGFR Mutants with Selectivity over Wild-Type EGFR. J Med Chem, 60, 3002-3019.
[23] Zhao, Z., Xie, L., Bourne, P. E. (2019). Structural Insights into Characterizing Binding Sites in Epidermal Growth Factor Receptor Kinase Mutants. J Chem Inf Model, 59(1), 453-462.
[24] Purba, E. R., Saita, E. I., Maruyama, I. N. (2017). Activation of the EGF receptor by ligand binding and oncogenic mutations: The "rotation model". Cells, 6(2), 1-19.
[25] Alzain, A. A., Almogaddam, M. A., Yousif, R., Alqarni, M. H., Foudah, A. I., Osman, W., et al. (2025). Molecular Docking, Molecular Dynamics Simulation, and Pharmacophore-Based Virtual Screening Unveil Natural Compounds with TIM-3 Inhibitory Activity. J Pharm Bioallied Sci, 17(2), S1882-S1887.
[26] Alsaady, I. M., Gattan, H. S., Aljahdali, S. M., Alruhaili, M. H., Dwived, V. D., Azhar, E. I. (2026). Conformational dynamics and binding free energy analyses unveil a stable flavonoid inhibitor of dengue virus NS5 polymerase. Scientific Reports, 16(1), 7761.
[27] Nurlelasari, N., Firdaus, A. R. R., Harneti, D., Indrayati, N., Baroroh, U., Yusuf, M. (2020). Computational study of the potential molecular target for antibreast cancer activity of limonoid derivatives from chisocheton SP. J Appl Pharm Sci, 10(2), 7-12.

[28] Isa, M. A, Kappo, A. P. (2025). Exploring phytoconstituents through molecular dynamics simulation: uncovering potential inhibitors for multiple targeted pathways in breast cancer. J Proteins Proteom, 16, 125-140.
[29] Sharanya, C. S., Sasikala, W. D., Sathi, S. N., Natarajan, K. (2024). Computational screening combined with well-tempered metadynamics simulations identifies potential TMPRSS2 inhibitors. Scientific Reports, 14(1), 16197.
[30] Dauda, G., Olorukooba, A. B., Adebisi, I. M., Ogundele, O. I., Jibril, M. M., Igharo, A. K., et al. (2026). Molecular docking and dynamics identify novel high-affinity plasmepsin II inhibitors from neem phytochemicals for antimalarial drug development. Discover Chemistry, 3(6), 1-26.
[31] Sahihi, M., Faraudo, J. (2022). Molecular Dynamics Simulations of Adsorption of SARS-CoV-2 Spike Protein on Polystyrene Surface. J Chem Inf Model, 62(16), 3814-3824.
[32] Sinha, P., Yadav, A. K. (2023). In silico identification and molecular dynamic simulations of derivatives of 6,6-dimethyl-3-azabicyclo[3.1.0]hexane-2-carboxamide against main protease 3CLpro of SARS-CoV-2 viral infection. J Mol Model, 29(130), 1-12.
[33] Alisaac, A. (2025). In silico analysis of quorum sensing modulators: Insights into molecular docking and dynamics and potential therapeutic applications. PLOS One, 20(6), 1-27.
[34] Mahfud, R. (2024). Molecular Dynamics Computational Study of Sustainable Green Surfactant for Application in Chemical Enhanced Oil Recovery. ACS Omega, 9(25), 27177-27191.
[35] Frimayanti, N., Nasution, M. R., Etavianti, E. (2021). Molecular docking and molecular dynamic simulation of 1,5-benzothiazepine chalcone derivative compounds as potential inhibitors for Zika virus helicase. Jurnal Riset Kimia, 12(1), 44–52.
[36] Singh, M. B., Jain, P., Tomar, J., Kumar, V., Bahadur, I., Arya, D. K., et al. (2022). An In Silico investigation for acyclovir and its derivatives to fight the COVID-19: Molecular docking, DFT calculations, ADME and td-Molecular dynamics simulations. Journal of the Indian Chemical Society, 99(5), 100433
[37] Nguyen, V. K. T., Camproux, A. C. (2025). Computational modeling of protein – ligand interactions: From binding site identification to pose prediction and beyond. Current Opinion in Structural Biology, 95, 1-3
[38] Irsal, R. A. P., Gholam, G. M., Firdaus, D. A., Liwanda, N., Chairunisa, F. (2024). Molecular Docking and Dynamics of Xylocarpus granatum as A Potential Parkinson's Drug Targeting Multiple Enzymes. Borneo Journal of Pharmacy, 7(2), 161–71.